Mathematical and Computational Applications, Vol. 15, No. 1, pp. 66-78, 2010.

NEURAL NETWORK MODEL FOR MOMENT-CURVATURE RELATIONSHIP OF REINFORCED CONCRETE SECTIONS

Muhiddin Bağcı
Civil Engineering Department, Celal Bayar University,
Manisa, Turkey. Muhiddin.bagci@bayar.edu.tr

Abstract- The analysis of moment-curvature relationship of reinforced concrete sections is complex due to large number of variables as well as non-linear material behavior involved. Artificial Neural Networks (ANNs) are found to be a tool capable of solving such problems. This has led to increasing use of ANN for analyzing the behavior of reinforced concrete sections. This paper reports the details of a study conducted using ANN for predicting moment-curvature relationship of a reinforced concrete section. Using data generated based on the analytical solutions, the ANN model was trained. The trained model was tested for a different set of input parameters and the output values were compared with the values based on analytical results. The agreement was found to be good.

Key Words- Moment-Curvature, Neutral Network

1. INTRODUCTION

The moment curvature for a cross-section envelope describes the changes in force capacity with deformation during a nonlinear analysis. The relationship between moment and curvature demonstrates the strength, ductility, energy dissipation capacity and rigidity of the section under question. To obtain the moment-curvature relationship of reinforced concrete section, various researchers have investigated using different models. Parviz [1] used firstly the filament method. Ersoy and Özcebe [2] presented a computer program to determine moment-curvature relationships of confined concrete sections. Artificial neural networks (ANN) are one of the artificial intelligence (AI) applications which have recently been used widely to model some of human interesting activities in many areas of science and engineering. The generalized delta rule algorithm of artificial neural networks is employed to predict the flexural behavior of Steel Fibre Reinforced Concrete (*SFRC*) T-beams using a computer program developed using C++ by Patodi and Purani [3]. For some other examples of ANN applications in structural analysis, the reader is referred to Jadid *et al.* [4] ; Berke *et al.* [5] ; Lee *et al.* [6]; Avdelas *et al* [7]; Abdalla and Stavroulakis [8]; Karlık *et al.* [9]. As far as structural analysis and design are concerned, Hajela *et al.* [10] used BPNN to represent the force-displacement relationship in static structural analysis. Jenkins considered the application of neural nets to approximate structural analysis and especially to a comparatively simple structure [11]. Mukherjee *et al.* [12] mapped the relationship between the slenderness ration, the modulus of elasticity and the buckling load for columns. As the input taken directly from the experimental results, factors affecting the buckling load of columns are automatically incorporated in the model to a great extent. Adeli defined the learning parameters as a function of iteration number of the training [13].

In this study, the behavior values of reinforced concrete sections subjected to flexure and axial load were obtained by using an analytical solution named the filament model, and then the required data for the network training were prepared. To obtain the behavior of confined concrete, several data points were used in training a multi-layer, feed-forward and back propagation artificial neural network (*ANN*) algorithm. The behavior values were calculated using the neural network and were compared with those obtained from the analytical results. Finally, the reliability of the ANN solution was validated by comparing experimental values with modeled values.

2. MATERIAL MODELS

Moment-curvature analysis for a reinforced concrete section, indicating the available flexural strength and ductility can be carried out provided that the stress-strain relationships for the concrete and steel reinforcements are known. Typical stress–strain curves for concrete are shown in Fig. 1.

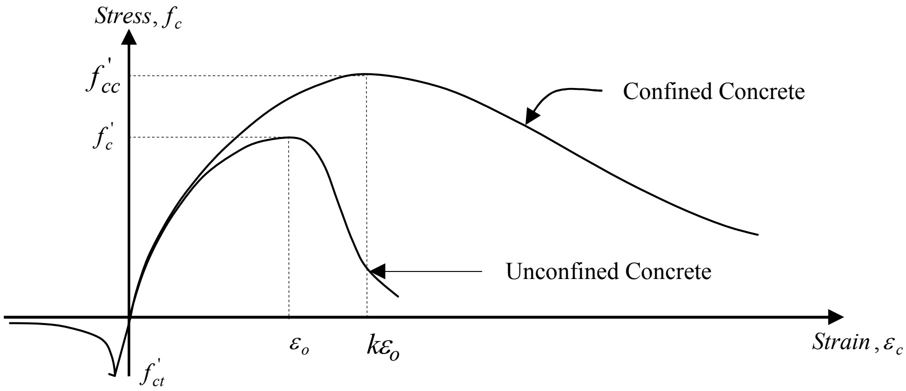

***Fig. 1**. Typical concrete stress-strain curve*

The material model for concrete used in this analysis is based on a model suggested by Modified Kent–Park [14]. This model takes into account the different stress-strain curves for unconfined and confined concrete as shown in Fig. 2. The general shape of curve is modeled by a second degree parabola for the ascending branch up to the maximum stress which corresponds to strain level of 0.002 and linear horizontal part leading to the ultimate strain.

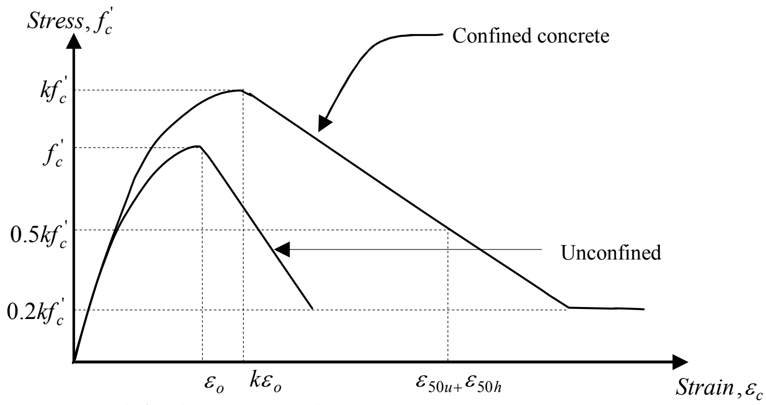

***Fig. 2**. Modified Kent-Park concrete stress-strain curve.*

In the ascending branch, the concrete compressive stress, f_c, at a given strain, ε_c is given by:

$$f_c = kf_c^{'}\left[2\left(\frac{\varepsilon_c}{\varepsilon_o k}\right)-\left(\frac{\varepsilon_c}{\varepsilon_o k}\right)^2\right] ; \qquad \varepsilon_c \le k\varepsilon_o \tag{1}$$

where $f_c^{'}$ is the concrete compressive strength and ε_o is concrete strain at the maximum stress assumed to be 0.002. It can be seen from Eq. (1) that concrete reaches a maximum stress of $kf_c^{'}$ at a strain of $k\varepsilon_o$. k is a factor which accounts for the strength increase due to the confinement. The value of the parameter k is obtained from;

$$k = 1 + \frac{\rho_s f_{yh}}{f_c^{'}} \tag{2}$$

where f_{yh} is the yield strength of stirrups, and ρ_s is the ratio of the volume of hoop reinforcement to the volume of concrete core measured to the outside of stirrups. The descending branch of the stress–strain curve is described as follows;

$$f_c = kf_c^{'}\left[1 - Z_m\left(\varepsilon_c - \varepsilon_o k\right)\right] \ge 0.2 f_c^{'}; \qquad \varepsilon_c > k\varepsilon_o \tag{3}$$

where

$$Z_m = \frac{0.5}{\varepsilon_{50u} + \varepsilon_{50h} - \varepsilon_o k} \tag{4}$$

$$\varepsilon_{50u} = \frac{3 + 0.285 f_c^{'}}{1.42 f_c^{'} - 1000} \tag{5}$$

$$\varepsilon_{50h} = 0.75 \rho_s \sqrt{b^{"} / s} \tag{6}$$

The term ε_{50u} defines the slope of the falling branch of the unconfined concrete, which identifies the strain at which the stress has fallen to $0.5kf_c^{'}$. The ε_{50h} is the additional ductility in concrete which is provided by transverse reinforcement. The “b” is the width of the confined core measured to the outside of stirrups, and s is the center to center spacing of stirrups or hoop sets. At large strains, the value of compressive stress is kept constant at $0.2kf_c^{'}$ to account for the ability of concrete to support load at large strains.

When a reinforced concrete member is subjected to tensile strains less than the cracking strain of concrete, the stress-strain relationship is approximately linear. A bi-linear model is used for concrete in tension. Rüsch [15] recommends the following relationship:

$$f_{c\,tention} = -E_{ct}\varepsilon_{ct} ; \qquad 0 \le \varepsilon_t \le \varepsilon_{c\,t} \tag{7}$$

$$f_{c\,tension} = f_{ct} - 5000 f_{ct}\left(\varepsilon_{ct} - 1000\right); \qquad \varepsilon_t \ge \varepsilon_{c\,t} \tag{8}$$

where E_{ct} is the modulus of elasticity in tension, ε_{ct} is the tensile strain. c_1 is taken as 0.5, ε_{cto} as 0.0001 and ε_{ctu} as 0.0002. The relationships given in Eq. (7) and Eq.(8) are shown in Fig. 3.

A sample reinforcement stress–strain relationship is shown in Fig.4. The constitutive model used for steel reinforcement is a simple elastic-plastic three linear model. These are the linear segment, the yield plateau, and the strain hardening segment. There are some other parameters of the reinforcement stress–strain relationship, such as the reinforcement yield strength , f_{yk} , the ultimate reinforcement strength, f_{su} , the reinforcement yield strain, ε_{sy} , hardening strain , ε_{st} , the ultimate strain, ε_{su} , and modulus of elasticity , E_s .

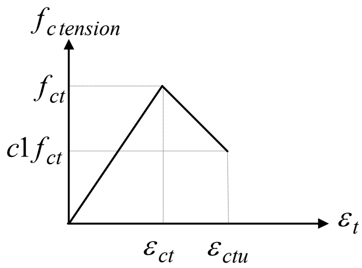

***Fig. 3**. Tension model for RC*

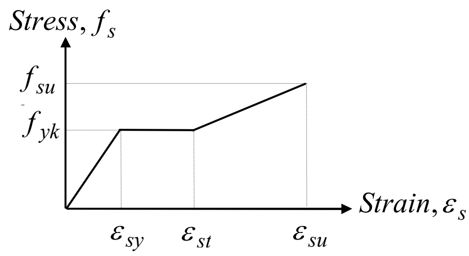

***Fig. 4**. Idealized reinforcement stress-strain curve*

3. METHOD OF ANALYSIS

The reinforced concrete section is modeled using filament method. As can be seen from Fig. 5, the cross-section is divided into 40 filaments to determine a moment-curvature relationship. For each filament, confined core and unconfined cover areas are defined. For a given strain at the extreme fiber in compression, the depth of neutral axis satisfying the force equilibrium is found by trial. For each filament, the average stresses are calculated at the centroids of unconfined and confined portions of the filament. To achieve this, first *the* strain at the centroids of the filament is calculated using the compatibility requirements. This centroidal strain is later used along with the appropriate concrete models to calculate stresses acting on the unconfined and confined portions of the filament. Finite concrete forces for the confined and unconfined portions of the filament (ΔF_{cc} and ΔF_{cu} respectively) are given multiplying the stress with the corresponding areas as follows:

$$\Delta F_{cu} = f_{cui} \cdot A_{cui} \tag{9}$$

and

$$\Delta F_{cc} = f_{cci} \cdot A_{cci} \tag{10}$$

where f_{cci} and f_{cui} are the concrete stresses for the confined and unconfined portions of the layer *i*.

Stress in the reinforcement at a given level is found by entering the f-ε diagram of steel with the strain value found from the compatibility requirements. Steel force at that level is given by multiplying the stress found with the area of the reinforcement at that level as:

$$F_{si} = \sigma_{si} A_{si} \tag{11}$$

This algorithm is demonstrated in Fig. 5 where only some typical finite forces are shown.

The moment-curvature relationship for a given axial load is determined by step by step incrementing concrete strain in the extreme compression fibre ε_{cm}. For each value of ε_{cm}, the strain gradient, i.e. the curvature φ, is obtained by satisfying the force equilibrium equation. The bending moment M corresponding to chosen value of ε_{cm} and axial load N are determined by taking moments of the internal forces about the geometric centroids of the section.

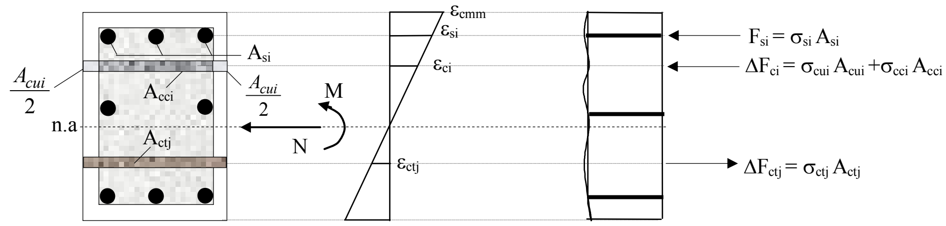

Fig. 5. *Strains and finite forces in the cross-section.*

4. PARAMETRIC STUDY

In this section the effect of different variables on flexural behavior are investigated using analytical solutions developed to predict the moment-curvature relationship of reinforced concrete cross-sections shown in Fig. 6.

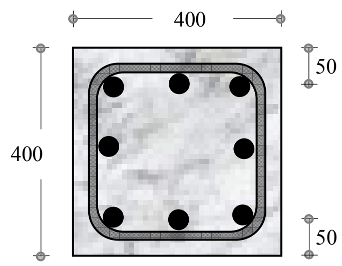

f_{ck} Characteristic strength of concrete (Mpa)
f_{yk} Yield strength of reinforcing steel (Mpa)
f_{sh} Yield strength of transverse steel (Mpa)
ε_{cu} Extreme fiber strain of unconfined concrete in compression .
ε_{cto} Strain of concrete in tension (0.0001)
ε_{ctu} Extreme strain of concrete in tension (0.0002)
ε_{sy} Yield strain of reinforcing steel (0.0021)
ε_{sh} Hardening Strain of reinforcing steel (0.01)
ε_{su} Extreme strain of reinforcing steel (0.1)

Fig. 6. *The cross-section considered in analyses.*

Table 1. *Results according to different variables*

No	*Variable properties*							*Curvature (rad/m)*				ε_{cm}	*M (kN-m)*
	f_{ck} *(Mpa)*	N/N_o *(N)*	f_{sh} *(Mpa)*	*s (cm)*	*Ø (mm)*	ρ	f_{yk} *(Mpa)*	*TY*	*TH*	*CvC*	*CoC*		
1	30	0	420	15	8	0.02	420	0.0085	0.0365	0.0321	0.0492	0.0125	241.0
2	20	0	420	15	8	0.02	420	0.0105	-	0.0245	0.0350	0.0125	228.2
3	16	0	420	15	8	0.02	420	0.0093	0.0363	0.0212	0.0323	0.0125	222.4
4	30	0.25	420	15	8	0.02	420	0.0112	-	0.0120	0.0141	0.0028	350.1
5	20	0.25	420	15	8	0.02	420	0.0171	-	0.0115	0.0125	0.0032	296.2
6	16	0.25	420	15	8	0.02	420	0.0167	-	0.0112	0.0118	0.0032	236.9
7	30	0.5	420	15	8	0.02	420	0.0251	-	0.0079	0.0089	0.0032	342.4

8	20	0.5	420	15	8	0.02	420	0.0264	-	0.0077	0.0081	0.0040	279.2
9	16	0.5	420	15	8	0.02	420	0.0263	-	0.0076	0.0079	0.0040	253.1
10	30	0.75	420	15	8	0.02	420	-	-	0.0078	0.0071	0.0028	246.1
11	20	0.75	420	15	8	0.02	420	-	-	0.0054	0.0065	0.0036	217.2
12	16	0.75	420	15	8	0.02	420	-	-	0.0048	0.0059	0.0036	173.8
13	30	0	420	15	8	0.011	420	0.0082	0.0338	0.0391	0.0648	0.0100	135.6
14	30	0	360	15	8	0.011	420	0.0082	0.0338	0.0391	0.0647	0.0100	135.5
15	30	0	300	15	8	0.011	420	0.0082	0.0337	0.0390	0.0646	0.0100	135.3
15	30	0	220	15	8	0.011	420	0.0082	0.0337	0.0390	0.0645	0.0100	135.0
17	30	0.25	420	15	8	0.011	420	0.0115	0.0520	0.0133	0.0151	0.0034	214.3
18	30	0.25	360	15	8	0.011	420	0.0115	0.0518	0.0133	0.0151	0.0032	213.7
19	30	0.25	300	15	8	0.011	420	0.0115	0.0515	0.0133	0.0150	0.0032	213.2
20	30	0.25	220	15	8	0.011	420	0.0114	0.0534	0.0132	0.0150	0.0032	212.6
21	30	0.50	420	15	8	0.011	420	0.0194	-	0.0082	-	0.0038	229.1
22	30	0.50	360	15	8	0.011	420	0.0193	-	0.0082	-	0.0038	227.2
23	30	0.50	300	15	8	0.011	420	0.0210	-	0.0081	-	0.0038	225.3
24	30	0.50	220	15	8	0.011	420	0.0208	-	0.0081	-	0.0038	222.7
25	30	0.75	420	15	8	0.011	420	-	-	0.0057	-	0.0030	172.7
…	…..	…..	…..	….	…..	…..	….	…..	…..	…...	…...	…….	…..
50	30	0.5	420	15	8	0.011	220	0.0104	-	0.0084	0.0094	0.0028	196.7
51	30	0.75	420	15	8	0.011	320	0.0151	-	0.0058	0.0065	0.0030	163.7
52	30	0.75	420	15	8	0.011	220	0.0124	-	0.0059	0.0067	0.0030	157.8

The results of the parametric study on reinforced concrete members presented here allow the following conclusions to be drawn.

1- As the compressive concrete strength increases, the tendency toward a brittle, sudden failure also increases. One of the disadvantages of a high-strength concrete is that it is more brittle than a concrete of a lower strength. The increasing compressive strength causes a decrease in ductility. The compressive strength, $f_{ck,}$ does not have any effects on the behavior in the case of pure bending. The compressive strength becomes effective with increasing axial load. The maximum moment capacity changes ±25% due to ±25% compressive strength variation.

2- The ductility decreases as level of the axial load increases. The variation of ductility with the level of axial load is quite significant. It is interesting to note that, although the sections considered are well confined, the behavior becomes very brittle under high levels of axial load. The upper limits imposed on axial loads in seismic codes roots from such considerations.

3- It is found that yield strength of transverse reinforcement, f_{sh}, has no effect on the behavior at all levels of the axial load.

4- The most important parameters for obtaining a ductile behavior are spacing of the confinement and the reinforcement configuration. Generally, closer confinement spacing and a denser reinforcement configuration does not contribute to a higher load capacity. The results presented in this study show that for a well-confined cross-section it is an advantage to use a higher grade of steel, while for a lightly confined section it is not. Table 1 shows that closer confinement spacing has little effect on maximum load. However, by decreasing the reinforcement confinement spacing a less brittle behavior can be achieved. From these tables it can be seen that the greatest effect of confinement is gained in pure compression.

5- To achieve ductility, the transverse reinforcement volume ratio needs to be increased and the reinforcement configuration should be designed to provide high confinement. As can be seen from Table 1, the increase in ductility with transverse reinforcement diameter has no significant effect on moment capacity. The crushing of core concrete delays with an increase in the diameter of transverse reinforcement. The diameter of transverse reinforcement becomes effective with the increasing axial load.

6- The reinforcement volumetric ratio, ρ has an important effect on the behavior of the confined section. The reinforcement volumetric ratio has significant effect on the behavior at low level axial load. The ultimate moment capacity increases from 10 % up to 30 % with the reinforcement volumetric ratio. The moment capacity decreases with the higher axial load. The reinforcement volumetric ratio is not effective on ductility.

7- The ductility increases remarkably when the reinforcement yield strength is increased with reinforcement configuration. The reinforcement yield strength, $f_{yk,}$, is an effective parameter in case of pure bending. The ultimate moment capacity changes from ±10 % up to ±30 % with the reinforcement yield strength.

5. ANN MODELING

Artificial Neural Networks (ANNs) approach is used to determine the behavior of confined concrete sections in this study. ANNs do not require an explicit understanding of the mechanism underlying the process, which is the main advantage. It has the capacity to learn the relationship between input and output provided that sufficient data are available for its training. The analytical results available for the confined sections were used to prepare the training and testing data sets for the network.

The present study is concerned with the prediction of a confined section using ANN. In this study a neural network program model developed by Karlık [9] in PASCAL was used. The data for training and testing were formed using parametric results. For generating the data analytically, filament method is used. The database consists of 52 sets of results, of which 45 sets were used for training the network, and the remaining 7 were used for testing in Table 1.

The training patterns should be normalized before they are applied to the neural network so as to limit the input and output values within a specified range. This is due to the large difference in the values of the data provided to the neural network. Besides, the activation function used in the back propagation neural network is a sigmoid function. The lower and upper limits of this function are 0 and 1, respectively. The following formula is used to pre-process the input data sets whose values are between 0 and 1.

$$v = \frac{x - x_{\min}}{x_{\max} - x_{\min}} \qquad [12]$$

Since the output value of the sigmoid function is between 0 and 1, the following function might be used. The combinations momentum rates {0, 0.3, 0.5, 0.7, and 0.9} are used to investigate their effects on the behaviour of the neural network convergence. The results are shown in Fig.7. The effects of all the given learning parameters and momentum rates on the convergence epoch and generalization of the neural network are shown in Table.2.

$$o = \frac{t - t_{\min}}{t_{\max} - t_{\min}} \qquad [13]$$

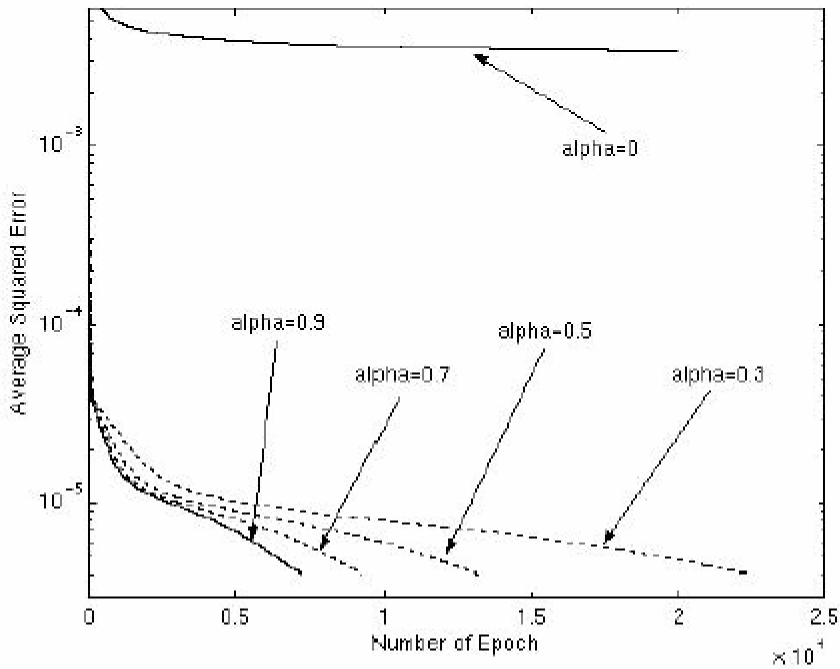

***Fig.7*.** Effect of Momentum Rate on the Training of Neural Network

Table.2. Effect of Learning and Momentum Rate on the Behaviour of Neural Network

Momentum factor	Behaviour of Neural Network	Learning rate %
0.9	Training of the neural network	7.82
	Generalizations for test patterns	3.7

The parametric study was conducted to find out the optimum number of hidden layers as well as the number of nodes for the present problem. The results of the parametric study conducted were shown in Fig.8. Training for all these network configurations was carried out initially for one thousand cycles with error tolerance value of 0.025. When the number of hidden layers was made two, only the architecture 12-13 reached the smallest error tolerance in 1000 cycles. With one hidden layer, the architecture was not able to attain the required error tolerance of 0.0065 within 1000 cycles. Hence, for the problem under consideration, the network with 2 hidden layers having the 12-13 architecture was chosen since it reaches the required error tolerance with the least number of cycles, which in turn would reduce the CPU time requirement.

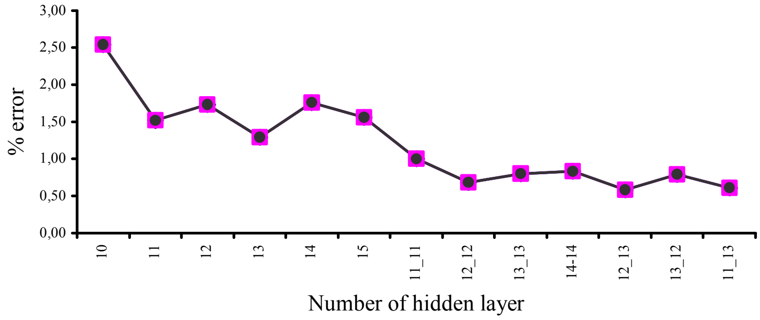

Fig. 8. *The error changes due to the number of nodes in the hidden layer at 1000 iterations.*

Using the 7-12-13-6 architecture in Fig.9, the network was trained and then tested. For training the network, totally 45 data set were used which were listed under Table 3. These input data sets were analytically generated using the filament model. The network, after being trained, was tested with 7 data sets. These 7 input data sets were formerly generated using the filament model. The remaining data sets used for testing the network are shown in Table 4.

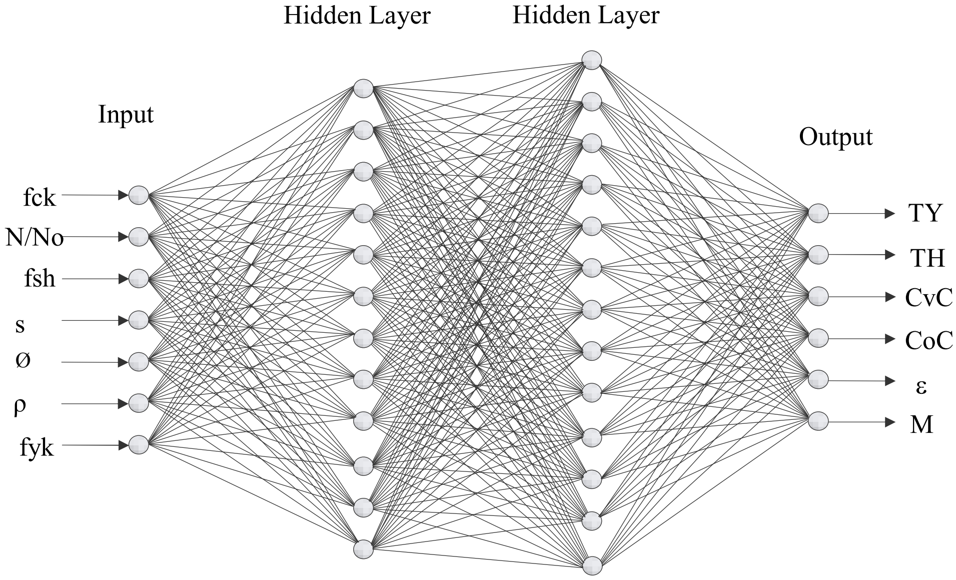

Fig. 9. *ANN architecture*

Finally, the least required error convergence for 7-12-13-6 architecture was reached within 5000 cycles. A numerical study of training and testing of the network was conducted keeping the error tolerance values as 0.1, and 0.001. For an error tolerance of 0.1, the number of cycles required is less; but the results are less accurate. In the case of 0.001, even though the accuracy is high, the numbers of cycles required are very high. Hence, keeping in mind the number of cycles required for convergence together with the accuracy needed for training and testing, the minimum error tolerance was chosen as 0.7% in Fig. 10

The training results predicted using ANN is compared with the parametric values in Table 2. In these cases, results represent a one to one correspondence, that is, the predicted and the parametric values are identical. The average error between the analytical and the ANN values ($\dfrac{|analytical\ - ANN| / ANN}{number\ \ of\ \ solution}$) produced is less than 0.2 %. The maximum differences between the analytical and ANN for TY, TH, CvC, CoC,ε and M are the outputs 0.965, 0.978, 1.039, 0.961, 0.962, and 0.976, respectively. Technically speaking, these errors are regarded to be sufficiently low.

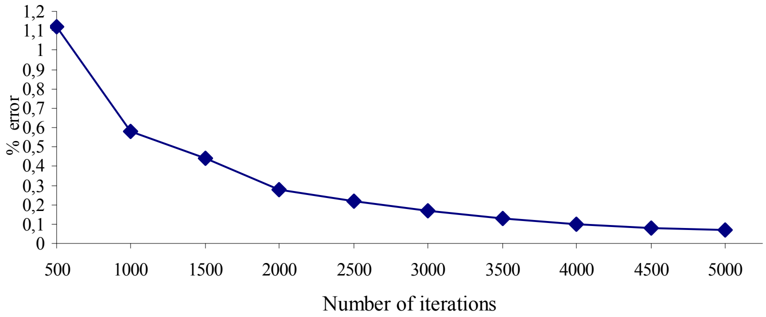

Fig. 10. *The error change at optimum ANN architecture (7:12:13:6)*

Table 3. *Training process and results*

No	*Meth.*	*TY*	Anal / *ANN*	*TH*	Anal / *ANN*	*CvC*	Anal / *ANN*	*CoC*	Anal / *ANN*	*ε*	Anal / *ANN*	*M*	Anal / *ANN*
1	Analy. ANN	0.0085 0.0083	1,016	0.0365 0.0369	0,987	0.0321 0.0313	1,023	0.0492 0.0490	1,004	0.0125 0.0124	1,006	241.0 241.99	0,996
2	Analy. ANN	0.0105 0.0104	1,001	- -	-	0.0245 0.0243	1,006	0.0350 0.0351	0,995	0.0125 0.0126	0,988	228.2 228.86	0,997
5	Analy. ANN	0.0171 0.0170	1,004	- -	-	0.0115 0.0111	1,027	0.0125 0.0128	0,977	0.0032 0.0031	1,005	296.2 295.29	1,003
6	Analy. ANN	0.0167 0.0167	0,999	- -	-	0.0112 0.0115	0,966	0.0118 0.0118	0,993	0.0032 0.0032	0,993	236.9 238.05	0,995
8	Analy. ANN	0.0264 0.0264	0,999	- -	-	0.0077 0.0074	1,029	0.0081 0.0082	0,983	0.0040 0.0039	1,002	279.2 280.52	0,995
9	Analy. ANN	0.0263 0.0263	1,000	- -	-	0.0076 0.0076	0,996	0.0079 0.0077	1,023	0.0040 0.0040	1,000	253.1 252.7	1,002
10	Analy. ANN	- -	-	- -	-	0.0078 0.0078	0,992	0.0071 0.0073	0,969	0.0028 0.0028	0,994	246.1 246.14	1,000
11	Analy. ANN	- -	-	- -	-	0.0054 0.0054	0,996	0.0065 0.0064	1,009	0.0036 0.0035	1,004	217.2 217.03	1,001
13	Analy. ANN	0.0082 0.0082	0,998	0.0338 0.0334	1,011	0.0391 0.0388	1,005	0.0648 0.0659	0,983	0.0100 0.0099	1,005	135.6 135.74	0,999
14	Analy. ANN	0.0082 0.0082	0,991	0.0338 0.0335	1,008	0.0391 0.0387	1,010	0.0647 0.0655	0,987	0.0100 0.0100	1,000	135.5 135.04	1,003
16	Analy. ANN	0.0082 0.0083	0,985	0.0337 0.0334	1,006	0.0390 0.0386	1,010	0.0645 0.0653	0,987	0.0100 0.0100	0,999	135.0 133.11	1,014
18	Analy. ANN	0.0115 0.0114	1,008	0.0518 0.0513	1,008	0.0133 0.0135	0,984	0.0151 0.0153	0,981	0.0032 0.0032	0,988	213.7 212.29	1,007
19	Analy. ANN	0.0115 0.0113	1,010	0.0515 0.0517	0,994	0.0133 0.0133	0,995	0.0150 0.0153	0,977	0.0032 0.0031	1,026	213.2 211.2	1,009
20	Analy. ANN	0.0114 0.0115	0,985	0.0534 0.0518	1,011	0.0132 0.0130	1,013	0.0150 0.0151	0,988	0.0032 0.0031	1,028	212.6 212.25	1,002
21	Analy. ANN	0.0194 0.0196	0,985	- -	-	0.0082 0.0081	1,011	- -	-	0.0038 0.0038	0,994	229.1 230.16	0,995
22	Analy. ANN	0.0193 0.0199	0,968	- -	-	0.0082 0.0081	1,012	- -	-	0.0038 0.0038	0,991	227.2 228.16	0,996
…	…..	……	……	……	…..	….	…..	……	…….	……	……	……	……
50	Analy. ANN	0.0104 0.0104	0,995	- -	-	0.0084 0.0082	1,022	0.0094 0.0092	1,018	0.0028 0.0028	0,984	196.7 195.85	1,004
51	Analy. ANN	0.0151 0.0150	1,005	- -	-	0.0058 0.0060	0,963	0.0065 0.0067	0,961	0.0030 0.0030	0,997	163.7 164.71	0,994
52	Analy. ANN	0.0124 0.0125	0,992	- -	-	0.0059 0.0059	0,995	0.0067 0.0068	0,972	0.0030 0.0029	1,006	157.8 157.09	1,005

The trained model was tested for a different set of input parameters and the output values were compared with the values based on analytical results. Seven different input values were applied to the model for testing the training network and the results were obtained in milliseconds. A comparison of the test and analytical values is given in Table 4. The average error ($\frac{\left| analytical \ - ANN \right| / ANN}{number \ of \ solution}$) obtained is about 0.33 %. The maximum differences (analytical / ANN) for *TY*, *TH*, *CvC*, *CoC*, ε and *M* are about 0.967, 0.966, 0.972, 0.968, 0.991, and 0.992, respectively. Therefore, the results can be said to indicate that the trained NN models have achieved good performance.

***Table 4**. Testing process and results*

No	*Method*	*TY*	Anal / *ANN*	*TH*	Anal / *ANN*	*CvC*	Anal / *ANN*	*CoC*	Anal / *ANN*	ε	Anal / *ANN*	*M*	Anal / *ANN*
3	Analy. ANN	0.0093 0.0094	0.987	0.0363 0.0375	0.966	0.0212 0.0206	1.025	0.0323 0.0313	1.031	0.0125 0.0125	0.999	222.4 224.1	0.992
4	Analy. ANN	0.0112 0.0110	1.014	- -	-	0.0120 0.0122	0.976	0.0141 0.0145	0.968	0.0028 0.0027	1.004	350.1 348.1	1.005
7	Analy. ANN	0.0251 0..025	1.001	- -	-	0.0079 0.0081	0.972	0.0089 0.0086	1.032	0.0032 0.0032	0.997	342.4 342.3	1.000
12	Analy. ANN	- -	-	- -	-	0.0048 0.0046	1.024	0.0059 0.0057	1.021	0.0036 0.0035	1.002	173.8 174.0	0.994
15	Analy. ANN	0.0082 0.0083	0.986	0.0337 0.0335	1.004	0.0390 0.0386	1.009	0.0646 0.0654	0.988	0.0100 0.0100	0.999	135.3 134.1	1.008
17	Analy. ANN	0.0115 0.0115	0.992	0.0520 0.0513	1.012	0.0133 0.0135	0.979	0.0151 0.0154	0.975	0.0034 0.0034	0.991	214.3 214.7	0.998
24	Analy. ANN	0.0208 0.0215	0.967	- -	-	0.0081 0.0082	0.978	- -	-	0.0038 0.0038	0.991	222.7 224.4	0.992

Compared to conventional digital computing techniques, neural networks are advantageous because of their special features, such as the massively parallel processing, distributed storing of information, low sensitivity to error, their very robust operation after training, generalisation and adaptability to new information.

6. CONCLUDING REMARKS

In this study, a back-propagation neural network model was employed to predict the influence of various parameters on the behavior of reinforced concrete sections. A neural network model was applied to the data derived from the analytical solutions. The analytical model is based on a filament modeling technique and capable of taking into account the crushing of cover and core concrete, the strain hardening of steel and the effect of confinement on core concrete.

To reduce the computing time of microprocessor of the system, a new computer model, which replies in milliseconds, was developed based on ANN method. A multi-layer, back propagation and feed-forward ANN algorithm was used to train the data. The ANN algorithms are not able to replace the conventional analytical techniques completely since they need some key values for training. However, in the determination of reinforced cross-section behavior, they can be implemented as an efficient supplementary tool to reduce the computational cost drastically**.** Modeling process in neural network is more direct since there is no necessity to specify a mathematical relationship between the input and the output variables. The trained ANN was able to produce quick results for the reinforced cross-section behavior with the same degree of accuracy as the filament model analysis achieved under flexure and axial load. Therefore, the trained ANN may be used in practice for determining the reinforced cross-sections behavior as an alternative to the time consuming filament model analysis.

The ANN applications presented in this study have demonstrated the viability and feasibility of using analytical results for the reinforced confined sections' behavior. The obtained results have shown that the neural network model is successful in modeling the non-linear relationship between different input and output parameters even when it involves a relatively smaller number of training patterns. It is envisaged that the model developed may be used in practical structural engineering applications.

7. REFERENCES

1. S. Parviz, S. Jongsung and W. H . Jer, Axial / Flexural Behavior of Reinforced Concrete Sections: Effects of Design Variables, *ACI*, **88**, 17-21, 1991.
2. U. Ersoy and G. Özcebe, Moment-Curvature Relationship of Confined Concrete Sections, *First Japan-Turkey Workshop On Earthquake Engineering*, Ankara, Turkey, 10-21,1997.
3. S. C. Patodi and V. S. Purani, Modeling flexural behavior of steel fibre reinforced concrete beams using neural networks, *Journal of New Building Materials and Construction World*, **4,** 28-35, 1998.
4. M. N. Jadid and D.R. Fairbairn, Neural-network applications in predicting moment-curvature parameters from experimental data, *Engineering Applications of Artificial Intelligence*, **9**, 309-319,1996.
5. L. Berke and P. Hajela, Applications of artificial neutral nets in structural mechanics, *Structural Optimizations*, **4**, 90-9, 1992.
6. Y. Lee, S. H. Oh, H. K. Hong and M. W. Kim, Design rules of multi-layer perception, *Proc. SPIE, Science of Artificial Neutral Nets in Structural Mechanics. Structural Optimization*, **1710,** 329-339, 1992.
7. A. V. Avdelas, P. D. Panagiotopoulos and S. Kortesis, Neutral networks for computing in the elastoplastic analysis of structures, *Meccanica*, **30**,1-15, 1995.
8. K. M. Abdalla and G. E. Stavroulakis, A Back propagation neutral network model for semi-rigid steel connections, *Microcomputers in Civil Engineering*, **10**, 77-87, 1995.
9. B. Karlık, E. Ozkaya, S. Aydın, S. and M. Pakdemirli, Vibration of beam -mass systems using artificial neutral networks, *Computers & Structures,* **69,** 339-347, 1998.
10. P. Hajela, and L. Berke, Neurobiological computational models in structural analysis and Design, *Computers & Structures*, **41,** 657-667, 1991.
11. W. M. Jenkins, An Introduction to Neural Computing for the Structural Engineer. *The Structural Engineer,* **75,** 38-4,. 1997.
12. A. Mukherjee, J. M. Deshpande and J. Anmala, Prediction of Buckling Load of Columns Using Artificial Neural Networks. *Journal of Structural Engineering,* **122***,* 1385-1387, 1996.

13. H. Adeli and H.S. Park, Counter propagation Neural Networks in Structural Engineering. *Journal of Structural Engineering,* .**121,** 1205-1212, 1995.
14. R. Park, M. J. N. Priestly and W. D. Gill, Ductility of square confined concrete columns, *Journal of Structural Division*, *ASCE*, **108**, 929–950, 1992.
15. H. Rüsch and H. Hilsdrof, *Verfomungei-genschaften von beton unter zentrishcen zugspannangen, Materialprüfungsemt für das bauwesen der technischen hochshule München,* 1963.